

## LEED and photoemission study of the stability of VO<sub>2</sub> surfaces

E. Goering, M. Schramme, O. Müller, R. Barth, H. Paulin, and M. Klemm  
*University of Augsburg, Memminger Strasse 6, 86159 Augsburg, Germany*

M. L. denBoer  
*Hunter College of the City University of New York, New York, New York 10021*

S. Horn  
*University of Augsburg, Memminger Strasse 6, 86159 Augsburg, Germany*  
 (Received 13 August 1996)

We present low-energy electron-diffraction (LEED) and photoemission measurements of single-crystal surfaces of VO<sub>2</sub>, made possible using samples oriented and characterized *in situ*. LEED shows that the (100) surface has a (1×2) reconstruction, but the (110) and (101) surfaces have diffraction patterns consistent with those expected from termination of the bulk. The (001) surface is evidently unstable: gentle *in situ* heating of our samples causes faceting, while similar heating of cleaved single crystals results in irreversible changes in photoemission spectra, which we interpret as surface relaxation of (001) facets. At the metal-insulator transition, photoemission spectra of the nearly sixfold coordinated stable (110) and (101) surfaces change greatly, but spectra of the (001) surface change only slightly. We suggest a coupling between the electronic and structural instabilities of VO<sub>2</sub> may be responsible. [S0163-1829(97)10507-0]

### INTRODUCTION

The metal-insulator transition (MIT) in transition-metal oxides has attracted much interest over the last decade. This interest was renewed by the discovery of high-temperature superconductivity in copper oxides, which exhibit a MIT as a function of doping. Besides their potential value in applications, transition-metal oxides are valuable testing grounds for basic research, since they appear to belong to the class of strongly correlated electrons, and the Hubbard model has been utilized to describe their properties. In particular, vanadium oxides are fascinating because the vanadium-oxygen phase diagram displays many compounds, with vanadium ions in various valence states, which exhibit MI transitions as a function of temperature. Most widely studied of these are V<sub>2</sub>O<sub>3</sub> and VO<sub>2</sub>, which show a MIT combined with a structural transition. While the transition in V<sub>2</sub>O<sub>3</sub> is often considered to be Mott-Hubbard, this is not completely clear for VO<sub>2</sub>.<sup>1,2</sup>

Photoelectron spectroscopy, which has proved to be a powerful tool in the investigation of correlated electron systems, has been carried out on VO<sub>2</sub>.<sup>3,4</sup> However, as photoemission is surface sensitive, and angle-resolved photoemission (which reveals the electronic properties in more detail than angle-integrated photoemission) requires atomically ordered single-crystal surfaces, a major difficulty in these measurements has been the lack of well-characterized, oriented surfaces. A standard procedure, *in vacuo* cleaving of single crystals, produces rough surfaces in the case of VO<sub>2</sub>.<sup>3,4</sup> Probably for this reason, to our knowledge, no previous low-energy electron diffraction (LEED) or angle-resolved photoemission investigations of VO<sub>2</sub> have been carried out. By adopting a strategy of gently heating, under suitable oxygen conditions, single crystals grown by chemical transport, we

have succeeded in obtaining VO<sub>2</sub> surfaces that we have used to obtain LEED patterns and angle-resolved photoemission measurements on this prominent compound. We observe large changes in the photoemission spectra at the metal-insulator transition, which shed light on the nature of the electronic states involved in this transition. In addition, our results help resolve inconsistencies between different authors in the photoemission literature on VO<sub>2</sub> concerning the intensity at the Fermi energy  $\epsilon_F$  and a feature in the spectra at a binding energy of about 10 eV. For example, Bermudez *et al.*<sup>3</sup> observed on cleaved single crystals time-dependent features at the bottom of the oxygen 2*p* band, which they interpreted as due to OH adsorbates, while the spectra of Shin *et al.*<sup>4</sup> have a different shape and do not exhibit time dependence. We show these inconsistencies are due to the instability of some VO<sub>2</sub> surfaces, which causes surface reconstruction and concomitant changes in the photoemission spectra.

### EXPERIMENT

VO<sub>2</sub> single crystals were grown in a gradient furnace by chemical transport reaction, using TeCl<sub>4</sub> as a transport agent. The growth temperature was ~600 °C. Under such conditions crystals close to the VO<sub>2</sub>/V<sub>8</sub>O<sub>15</sub> phase boundary are obtained, some of which show specular surfaces. Electrical resistivity and magnetic susceptibility measurements show the MIT at  $T_{MI}=340$  K. The crystal orientation was determined *ex situ* by Laue diffraction using a standard Philips x-ray Laue camera before introducing the crystals into the ultrahigh vacuum (UHV) chamber. Several cycles of heating to 600–700 K under suitable oxygen partial pressure then produced good quality LEED patterns; those presented be-

low were all measured in the rutile phase just above the MIT, using an Omicron Spectacleed system and software for contrast enhancement.

Ultraviolet photoemission (UPS) experiments using a He discharge lamp were performed in a mu-metal shielded system equipped with a VSW CLASS 100 analyzer. A total resolution of 20 meV could be achieved. Additional measurements were performed at beam line U4A of the NSLS at Brookhaven National Laboratory, using a toroidal grating monochromator operated in a constant resolution mode with a resolution of about 150 meV and overall resolution of 500 meV. In both systems the temperature could be varied between 80 and 1000 K and the base pressure was below  $10^{-10}$  mbar. Since the secondary electron background of the UPS spectra changes when passing through the MIT, all UPS spectra shown are background subtracted employing a Shirley-like method<sup>5</sup> introduced by Li and Henrich.<sup>6</sup> In addition, all spectra are normalized to the area under the spectra.

### RESULTS: LOW-ENERGY ELECTRON DIFFRACTION

In its metallic phase,  $\text{VO}_2$  forms the rutile structure with space group 136,  $P4_2/mnm$ ,<sup>7</sup> and lattice vectors  $a_r=b_r=4.551 \text{ \AA}$  and  $c_r=2.851 \text{ \AA}$ .<sup>8</sup> In this paper we refer all surface indices to this rutile structure. The main structural effect at the MIT is a dimerization of vanadium ions along the  $c_r$  axis, forming zigzag chains and doubling the unit cell along the  $c_r$  axis. This insulating phase has the  $\text{MoO}_2$  structure with space group  $P2_1/c$ .<sup>9,10</sup> We investigated the (100), (001), (110), and (101) surfaces in both the metallic and insulating phases.

#### (110) Surface

On this surface, six oxygen atoms coordinate each vanadium ion. Of the various low-index  $\text{VO}_2$  surfaces we have studied, this corresponds most nearly to the bulk coordination, and we therefore expect this surface to be the most stable, as also suggested by Henrich.<sup>11</sup> This belief is supported by superstructure calculations, based on linear combination of muffin tin-type orbitals, by Kasowsky and Tait<sup>12</sup> on isostructural  $\text{TiO}_2$ , which show no additional gap states on the projected surface density of states, in contrast to the  $\text{TiO}_2$  (001) surface, on which the same calculations show surface states in the gap region.

Figure 1(a) shows a section of the  $\text{VO}_2$  (110) surface terminated by the V ion plane. Axes referred to the rutile lattice are sketched on the figure. Small (large) spheres represent vanadium (oxygen) ions. The outermost layer of V ions is highlighted in white. Figure 1(b) shows a LEED pattern of this (110) surface oriented as in Fig. 1(a), taken at a sample temperature above the MI transition, i.e., in the rutile phase, with an incident electron energy of 55 eV. The LEED pattern shows a face centered structure whose surface unit cell is illustrated in Fig. 1(a). Quantitative analysis yields a real-space periodicity of  $3.6 \pm 0.7 \text{ \AA}$ , in agreement with  $d_{\text{VV}}$ , the distance between adjacent V ions at the bulk-terminated surface, which is  $3.52 \text{ \AA}$  [Fig. 1(a)]. This appears surprising since  $d_{\text{VV}}$  evidently differs from either of the  $\text{VO}_2$  surface lattice lengths. There are two V ions per unit cell, each with differing oxygen coordination. The absence of this periodic-

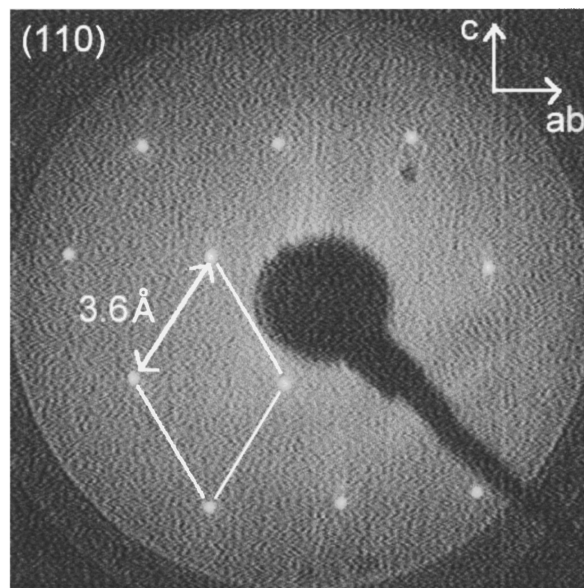
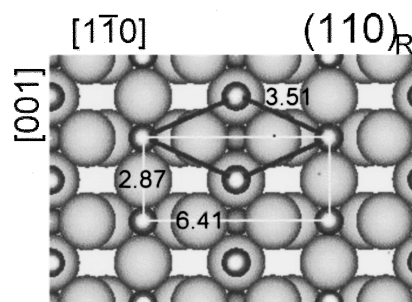


FIG. 1. (a) Projected bulk structure of the rutile (110) surface of  $\text{VO}_2$ . The  $c$  axis is up (toward top of page) and the  $ab$  diagonal is to the right. Small (large) spheres represent V (O). Outermost V ions are highlighted. (b) LEED pattern of (110)<sub>R</sub> surface of  $\text{VO}_2$ , oriented as in (a), at incident electron energy of 56 eV.

ity in the LEED pattern may be due to the fact that V has a much larger electron scattering cross section than O, so the scattering, and the observed LEED pattern, is dominated by the V sublattice. It must be noted, however, that LEED on the isostructural  $\text{TiO}_2$  (110) surface does show the bulk periodicity,<sup>13</sup> at least at a higher electron energy (92 eV). We observe large variations in the intensity of the individual reflections as a function of electron energy, but have not yet analyzed this quantitatively.

#### (101) Surface

The surface V-O coordination of the (101) surface should be similar to that of the (110) surface.<sup>11</sup> Evidence for the stability of this surface is the fact that single crystals grown by chemical transport show predominantly smooth (110) and (101) surfaces, terminated by rough (001) surfaces. We therefore expect that the (101) surface structure corresponds to the bulk structure, as found for the (110) surface.

In Fig. 2(a) we show a  $\text{VO}_2$  section, similar to that of Fig. 1(a), for the (101) surface, including axes with respect to the rutile structure. Figure 2(b) shows the corresponding LEED

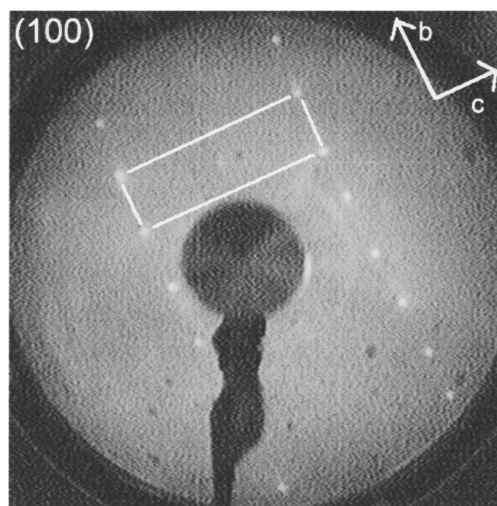
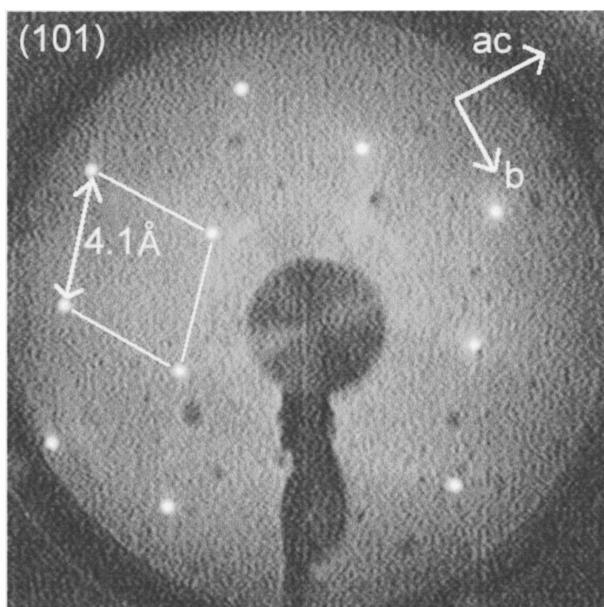
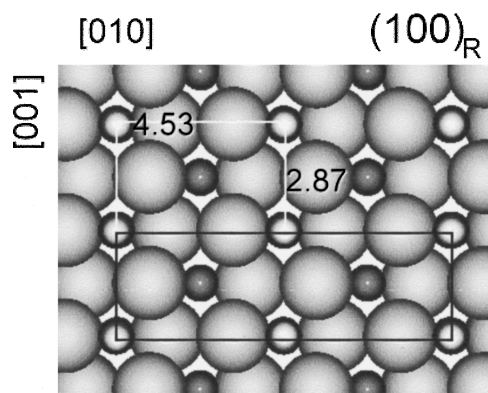
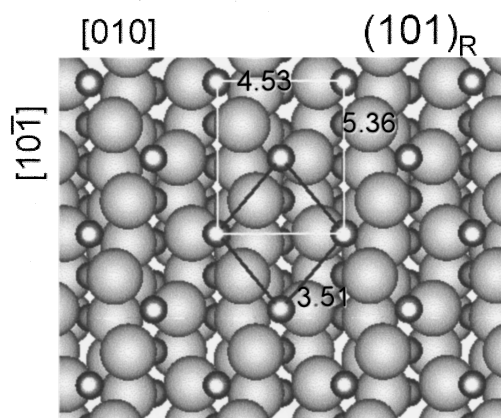


FIG. 2. (a) Projected bulk structure of the rutile (101) surface of  $\text{VO}_2$ . Small (large) spheres represent V (O). Outermost V ions are highlighted. (b) LEED pattern of  $(101)_R$  surface of  $\text{VO}_2$ , oriented as in (a), at incident electron energy of 44.3 eV.

pattern, rotated  $45^\circ$  clockwise. The face centered LEED pattern is similar to that of the (110) surface; quantitative analysis yields a measured surface unit cell length of  $4.1 \pm 0.8 \text{ \AA}$ , in agreement with the value of  $3.51 \text{ \AA}$  for  $d_{\text{vv}}$  expected from the bulk vanadium sublattice structure [Fig. 2(a)]. For this surface there are no theoretical or experimental studies of the corresponding  $\text{TiO}_2$  surface.

#### (100) Surface

We show in Fig. 3(a) a section of the (100) surface including again axes with respect to the rutile lattice. The darker V ions marked with a white dot, in the center of the vanadium rectangle, are  $\frac{1}{2} a$   $\mathbf{b}$  lattice constant ( $4.53 \text{ \AA}$ ) below the upper brighter V layer. The LEED pattern of this surface is shown in Fig. 3(b). The  $k$  space surface unit cell is indicated by the white lines. The LEED pattern is inconsistent with the face centered structure expected for the termination of the bulk structure: the ratio  $b/c$  is 3.2, almost twice as

FIG. 3. (a) Projected bulk structure of the rutile (100) surface of  $\text{VO}_2$ . Small (large) spheres represent V (O). Outermost V ions are highlighted. (b) LEED pattern of  $(100)_R$  surface of  $\text{VO}_2$  showing a  $(1 \times 2)$  reconstruction, oriented as in (a).

large as expected from the bulk structure (1.58), implying a  $(1 \times 2)$  surface reconstruction. The resulting surface cell in real space is shown in Fig. 3(a) (black rectangle).

Reconstructions of the (100) surface of isostructural  $\text{TiO}_2$  were observed by Chung, Lo, and Somorjai,<sup>13</sup> who found various modifications at different annealing temperatures  $T_A$ : a  $(1 \times 3)$  reconstruction at  $T_A = 500\text{--}600^\circ\text{C}$ ,  $(1 \times 5)$  at  $T_A = 800^\circ\text{C}$ , and  $(1 \times 7)$  at  $T_A = 1200^\circ\text{C}$ . From Auger spectroscopy, they concluded that oxygen loss from the surface region increased with increasing annealing temperature  $T_A$ . The observed reconstructions can be explained by a loss of oxygen rows along the rutile  $c$  axis. Figure 4 shows a surface model of the rutile (100) surface with a typical oxygen vacancy.<sup>11</sup> The topmost oxygen ions form chains along  $c_{\text{rut}}$ . The absence of every second oxygen row causes a  $(1 \times 2)$  reconstruction; the absence of two adjacent oxygen rows a  $(1 \times 3)$  reconstruction, etc. We are currently studying the possibility that such periodic oxygen loss occurs in  $\text{VO}_2$ .

#### (001) Surface

Brief heating of the (001) surface caused the appearance of a fourfold symmetric LEED pattern with a surface unit

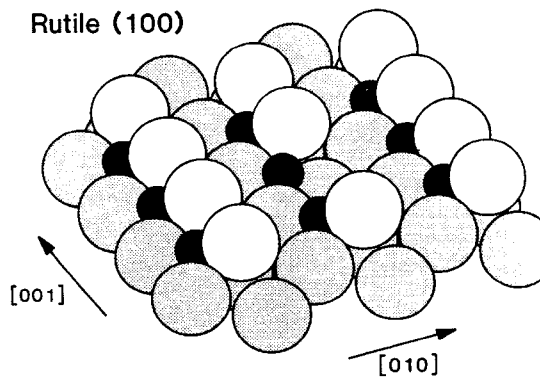


FIG. 4. VO<sub>2</sub> surface model; reproduced from Ref. 11.

cell length of  $4.9 \text{ \AA} \pm 0.8 \text{ \AA}$ , in agreement with the *a* (or *b*) lattice parameter of VO<sub>2</sub>. Further heating resulted in a complex LEED pattern consistent with faceting, behavior previously observed on the analogous TiO<sub>2</sub> (001) surface.<sup>12-14</sup>

### RESULTS: PHOTOEMISSION

We now discuss photoemission measurements on these single-crystal surfaces, focusing particularly on the effect of the reconstructions of the (100) surface just described. For comparative purposes, we describe spectra taken from surfaces produced by cleaving and by scraping VO<sub>2</sub> single crystals as well as those produced by heating in oxygen.

Figure 5 compares photoemission spectra taken with He II radiation from a VO<sub>2</sub> surface freshly cleaved at room temperature with those taken from the same surface heated above the MIT (to  $T=400 \text{ K}$ ) and after cooling back to room temperature again. The initial spectrum clearly differs from those taken after heating: raising the temperature above the MIT causes an irreversible reduction of density of states at

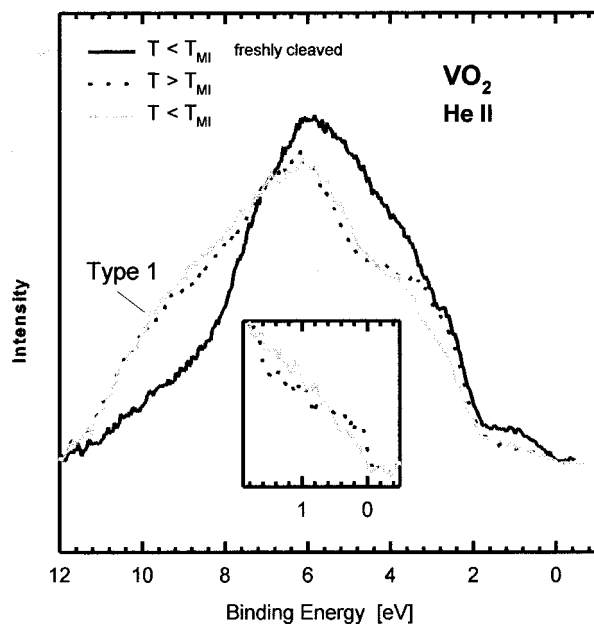


FIG. 5. Photoemission spectra (He II) of VO<sub>2</sub> surface produced by cleaving. Freshly cleaved (solid), above MIT (dotted), and after cooling to room temperature (grayed).

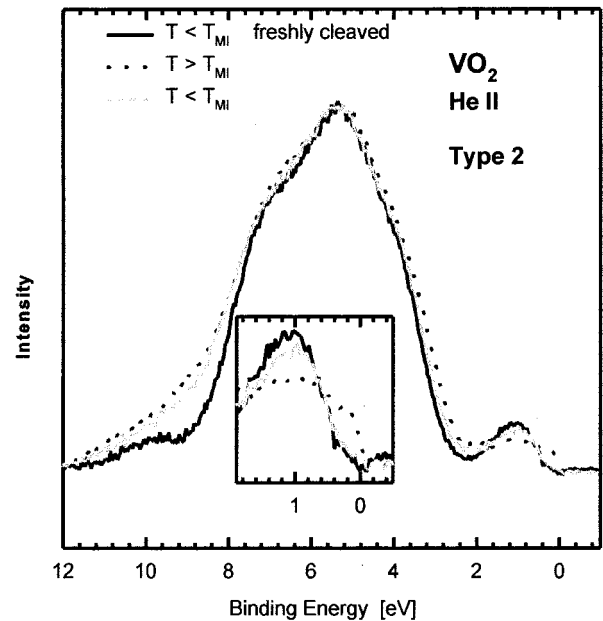


FIG. 6. Photoemission spectra (He II) of VO<sub>2</sub> surface produced by cleaving. Freshly cleaved (solid), above MIT (dotted), and after cooling to room temperature (grayed).

$\epsilon_F$  and the appearance of additional intensity at the bottom of the valence bands. Spectra having the shape of the latter we refer to in the following as “type 1” spectra. Although the O  $2p$  and V  $3d$  states are hybridized, following an early model of Goodenough<sup>15</sup> we can identify the features in the binding energy region from 12 to 2 eV as primarily of O  $2p$  character and those features in the region between  $\epsilon_F$  and 2 eV as primarily of V  $3d$  character. Figure 5 shows that a type 1 spectrum is characterized by additional intensity at the bottom of the O  $2p$  band at  $\sim 10$  eV binding energy and decreased intensity in the V  $3d$  band region. These changes develop on keeping the sample above  $T_{MI}$  for 5–10 min; the pressure remained less than  $5 \times 10^{-10}$  mbar while heating. A freshly cleaved sample kept at room temperature continues to show unchanged spectra for at least several hours. On the other hand, after a single brief (5–10 min) heating above the MIT, the sample exhibited only type 1 spectra. Subsequent heating above the MIT then causes only the appearance of the Fermi cutoff characteristic of a metal, although with very low intensity at  $\epsilon_F$ , and minor changes at the top of the O  $2p$  bands; the changes that heating above the MIT induces are evidently irreversible. The surface of the cleaved sample of Fig. 5 was rough and exhibited no LEED pattern either before or after heating.

Figure 6 shows three spectra taken from a surface produced by cleaving a different VO<sub>2</sub> crystal. The spectrum taken immediately after cleaving (solid line) is somewhat similar to the spectrum of the freshly cleaved sample of Fig. 5, which we henceforth refer to as type 2 spectra. When this sample is heated above the MIT ( $T=400 \text{ K}$ ), a well-defined Fermi cutoff appears, with much more intensity at  $\epsilon_F$  than in type 1 spectra, and, in further contrast to type 1 spectra, the intensity at the bottom of the O  $2p$  bands ( $\sim 10$  eV) increases only slightly. Cooling to room temperature (below  $T_{MI}$ ) causes the intensity at  $\epsilon_F$  to vanish and minor changes at the top of the oxygen bands. These changes are reversible when

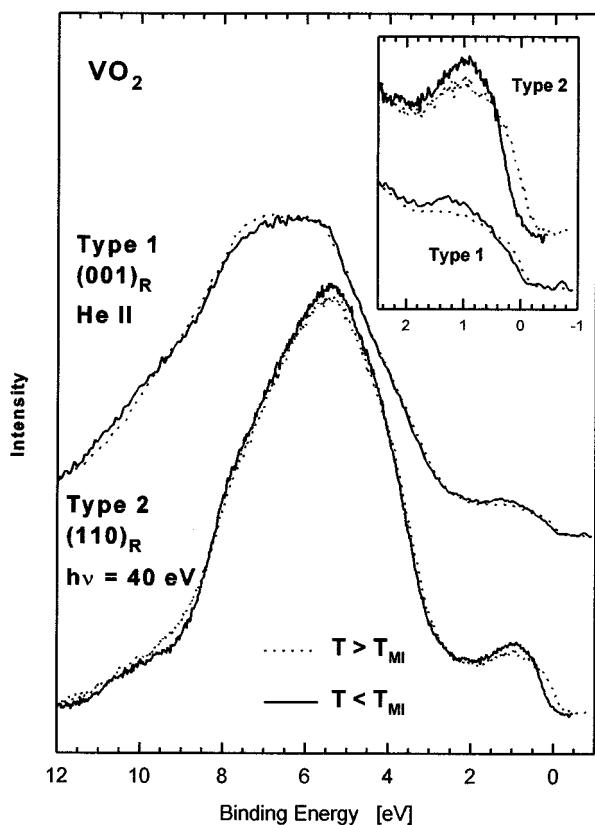


FIG. 7. Photoemission spectra of (001) and (110) surfaces of  $\text{VO}_2$  for  $T > T_{\text{MI}}$  and  $T < T_{\text{MI}}$ . Spectra of the (001) surface are of type 1, while those of the (110) surface are of type 2. The (001) spectra were measured with He II, while the (110) spectra were measured at U4A at 40 eV.

the sample is subsequently heated through the MIT.

To further investigate this behavior we compare these photoemission spectra of cleaved crystals, which do not show LEED patterns, with spectra of surfaces prepared by heating under oxygen, which showed the LEED patterns discussed above. Figure 7 shows spectra of the (001) and (110) surfaces of  $\text{VO}_2$  for  $T > T_{\text{MI}}$  and  $T < T_{\text{MI}}$ . [The (110) crystal was slightly doped with  $\text{MoO}_2$ , which does not affect the photoemission features but merely shifts the MIT to slightly lower temperatures.] It is evident from Fig. 7 that the (001) surface exhibits a type 1 spectrum, while the (110) surface exhibits a type 2 spectrum. The spectra of both surfaces change reversibly, and in the ways described above for type 1 and type 2 spectra, respectively, when the sample is repeatedly cycled through the MIT.

This apparent relationship between the surface plane and the spectral features provides a natural explanation of the different types of spectra observed for cleaved samples (Figs. 5 and 6). The sample displaying type 2 spectra above and below  $T_{\text{MI}}$  (Fig. 6) evidently consisted predominantly of (110) facets. The freshly cleaved sample of Fig. 5 showed spectra similar to those of the (001) face (Fig. 7) when heated above  $T_{\text{MI}}$ , suggesting that its surface then reconstructed toward that surface. The evident sensitivity of the photoemission spectra to the surface plane also clarifies differences between reported photoemission measurements on  $\text{VO}_2$ . Shin *et al.*<sup>4,16</sup> used single crystals with an optically

smooth (110) surface before cleaving. The surfaces were rough after cleaving, but in view of the initial orientation it is likely that they still consisted largely of (110) facets. Indeed, their spectra are very similar to our type 2 spectra, which are characteristic of the (110) face. Bermudez *et al.*,<sup>3</sup> on the other hand, used needlelike  $\text{VO}_2$  single crystals, which they broke perpendicular to the needle axis. Our experience with the growth of  $\text{VO}_2$  crystals indicates that such needles consist mainly of (110) and (101) surfaces perpendicular to the needle axis, which usually terminate in a (001) surface. The surfaces produced by breaking a needle should then consist mainly of (001) facets. Bermudez *et al.* measured in a defined hydrogen atmosphere to study the effect of hydrogen on the MIT.<sup>3</sup> Their spectra immediately after cleaving are similar to our type 2 spectra, and over time changed to spectra similar to our type 1. The authors attributed this change to OH diffusion along grain boundaries, by analogy to similar behavior observed for  $\text{V}_2\text{O}_3$  (Ref. 17) and  $\text{Ti}_2\text{O}_3$  (Ref. 18) on the absorption of water. However, the fact that similar changes occurred in our experiments, although the partial pressure of water was negligible, supports our interpretation of an intrinsic surface instability.

The LEED results show that each  $\text{VO}_2$  surface behaves like the corresponding  $\text{TiO}_2$  surface, suggesting analogous interpretations of the photoemission spectra of these surfaces. Tait *et al.*<sup>14</sup> have measured the photoemission spectra of annealed  $\text{TiO}_2$  (001). They found changes in their spectra on annealing similar to those we find for  $\text{VO}_2$  on annealing.

Band-structure calculations of  $\text{VO}_2$  (Refs. 19 and 20) show the lower part of the O  $2p$  bands is strongly hybridized with the V  $3d$  states. On the (001) surface of  $\text{VO}_2$  the V  $3d$  states, assuming the bulk structure, are partially filled due to the low oxygen coordination. Correspondingly there is emission from V  $3d$  states near  $\epsilon_F$  in the photoemission spectrum. The MIT is associated with a structural transition; there is therefore structural instability and phonon mode softening.<sup>21</sup> Applying a model that has been used with success for  $\text{TiO}_2$ ,<sup>11,14</sup> we suggest this instability could trigger surface relaxation, helping the surface V ions achieve an O coordination higher than on the unrelaxed surface. Such an increase in O coordination would decrease the occupancy of the V  $3d$  states, decreasing the V  $d$  intensity at  $\epsilon_F$  while increasing the intensity of emission from the bottom of the O  $p$  bands, as observed in our photoemission data when a cleaved (001) surface is heated above  $T_{\text{MI}}$  for the first time (Fig. 5). These changes in electron configuration correspond to the energy gain which drives the surface relaxation. The stable (110) surface, on the other hand, has higher V coordination and the occupied DOS in the V  $3d$  band region is higher than on the relaxed (001) surface. Therefore, the effect of the MIT on the DOS of the (110) surface at  $\epsilon_F$  is much higher. The stability of the (110) surface means that the changes in the photoemission spectra of that surface which occur at the MIT are associated with bulk properties and not with surface structural changes, as we suggest is the case for the (001) surface.

## CONCLUSIONS

We have succeeded in preparing and orienting single-crystal surfaces of  $\text{VO}_2$ , which show high-quality LEED pat-

terns and have measured photoemission on several low index planes. LEED shows that the (110) and (101) surfaces are stable, while the (001) surface shows faceting. The (100) surface relaxes, a relaxation associated with the MIT. We have shown that the corresponding observed photoemission spectra and their changes upon annealing as well as photoemission measurements described previously in the literature are consistent with a model previously developed for TiO<sub>2</sub>. While photoemission can contribute much to our understanding of the electronic structure and the nature of the metal-insulator transition in VO<sub>2</sub>, our measurements show the sen-

sitivity of such photoemission to surface geometry and morphology, and emphasize the need for careful characterization.

#### ACKNOWLEDGMENTS

This work was supported in part by the German DFG and the U.S. DOE. The NSLS is supported by the U.S. DOE, Division of Materials Sciences and Division of Chemical Sciences (DOE Contract No. DE-AC02-76CH00016).

- 
- <sup>1</sup>R. M. Wentzcovich, W. W. Schultz, and P. B. Allen, *Phys. Rev. B* **72**, 3389 (1994).  
<sup>2</sup>T. M. Rice, *Phys. Rev. Lett.* **73**, 3042 (1994).  
<sup>3</sup>V. M. Bermudez, R. T. Williams, J. P. Long, R. K. Reed, and P. H. Klein, *Phys. Rev. B* **45**, 9266 (1992).  
<sup>4</sup>S. Shin, S. Suga, M. Tanaguchi, M. Fujisawa, H. Kanzaki, A. Fujimori, H. Diamon, J. Ueda, K. Kosuge, and S. Kachi, *Phys. Rev. B* **41**, 4993 (1990).  
<sup>5</sup>D. A. Shirley, *Phys. Rev. B* **5**, 4709 (1972).  
<sup>6</sup>X. Li and V. E. Henrich, *J. Elect. Spectrosc. Relat. Phenom.* **63**, 253 (1993).  
<sup>7</sup>S. Westman, *Acta Chem. Scand.* **15**, 217 (1961).  
<sup>8</sup>D. B. McWhan, M. Marezio, J. P. Remeika, and P. D. Dernier, *Phys. Rev. B* **10**, 490 (1974).  
<sup>9</sup>A. Zylbersztejn and N. F. Mott, *Phys. Rev. B* **11**, 4383 (1975).  
<sup>10</sup>W. Brückner, *Kristall und Technik* **16**, K28 (1981).  
<sup>11</sup>V. E. Henrich, *Prog. Surf. Sci.* **14**, 175 (1983).  
<sup>12</sup>R. V. Kasowsky and R. H. Tait, *Phys. Rev. B* **20**, 5168 (1979).  
<sup>13</sup>Y. W. Chung, W. J. Lo, and G. A. Somorjai, *Surf. Sci.* **64**, 588 (1977).  
<sup>14</sup>R. H. Tait and R. V. Kasowky, *Phys. Rev. B* **20**, 5178 (1979).  
<sup>15</sup>J. B. Goodenough and H. Y.-P. Hong, *Phys. Rev. B* **8**, 1323 (1972).  
<sup>16</sup>A. Fujimori, *Physica B* **163**, 736 (1990).  
<sup>17</sup>R. Kurtz and V. E. Henrich, *Phys. Rev. B* **28**, 6699 (1983).  
<sup>18</sup>R. Kurtz and V. E. Henrich, *Phys. Rev. B* **26**, 6682 (1982).  
<sup>19</sup>O. Müller, Ph.D. dissertation, University of Augsburg, 1996.  
<sup>20</sup>E. Goering, Ph.D. dissertation, University of Augsburg, 1996.  
<sup>21</sup>F. Gervais and W. Kress, *Phys. Rev. B* **31**, 4809 (1985).